High Resolution Multispectral And Hyperspectral Data Fusion For Advanced Geospatial Information Products – Final Report

W. Paul Bissett
Florida Environmental Research Institute
10500 University Center Drive
Suite 140
Tampa, FL 33612

phone: (813) 866-3374 x102 fax: (813) 977-8057 email: pbissett@feriweb.org

David D. R. Kohler
Florida Environmental Research Institute
10500 University Center Drive
Suite 140
Tampa, FL 33612

Award Number: N00014-05-1-0416

phone: (813) 866-3374 x114 fax: (813) 977-8057 email: dkohler@feriweb.org

http://www.feriweb.org

LONG-TERM GOALS

This project seeks to develop the technology to fuse high spatial resolution MultiSpectral Imagery (MSI) with lower spatial resolution, but higher spectral resolution, HyperSpectral Imagery (HSI) to provided enhanced target detection and battlespace characterization. It seeks to push beyond traditional PAN sharpening techniques to develop applications that will increase the accuracy and fidelity of the sharpened spectral imagery.

OBJECTIVES

1) Co-register high resolution MSI data with HSI data collected during the Fall of 2004.

2) Correct the MSI data for illumination and atmospheric interference to derive a broadband remote sensing reflectance, Rrs, measurement from the MSI data.

3) Develop methodologies to fuse the HSI data with the higher spatial resolution MSI data, using the spectral characterization of the MSI Rrs data stream.

APPROACH

The fusion of remote sensing data from different sensors has a long history of success in the terrestrial environment (Pohl and Genderen, 1998). Its application in ocean remote sensing has accelerated in recent years with the use of multiple resolution, multiple frequency optical and microwave imaging. The optical imagers include both active (e.g. LIDAR) and passive (e.g. HyperSpectral Imagers, HSI).

REPORT DOCUMENTATION PAGE

Form Approved
OMB No. 0704-0188

1. REPORT DATE *(DD-MM-YYYY)*: 30-03-2007

2. REPORT TYPE: Final

3. DATES COVERED *(From - To)*: Mar 15, 2005--Dec 31, 2006

4. TITLE AND SUBTITLE

High Resolution Multispectral and Hyperspectral Data Fusion for Advanced Geospatial Information Products

5a. CONTRACT NUMBER

5b. GRANT NUMBER: N00014-05-1-0416

5c. PROGRAM ELEMENT NUMBER

6. AUTHOR(S)

W. Paul Bissett

5d. PROJECT NUMBER

5e. TASK NUMBER

5f. WORK UNIT NUMBER

7. PERFORMING ORGANIZATION NAME(S) AND ADDRESS(ES)

Florida Envoronmental Research Institute
10500 University Center Drive, Suite 140
Tampa, Florida 33612

8. PERFORMING ORGANIZATION REPORT NUMBER

9. SPONSORING/MONITORING AGENCY NAME(S) AND ADDRESS(ES)

Office of Naval Research
100 Alabama St SW
Suite 4R15
Atlanta, GA 30303-3104

10. SPONSOR/MONITOR'S ACRONYM(S): ONR

11. SPONSOR/MONITOR'S REPORT NUMBER(S)

12. DISTRIBUTION/AVAILABILITY STATEMENT

Approved for Public Release; Distribution is Unlimited

13. SUPPLEMENTARY NOTES

N/A

14. ABSTRACT

See Attached

15. SUBJECT TERMS

Hyperspectral Imagery (HSI), MultiSpectral Imagery (MSI),remote sensing, geo-positioning, panchromatic (PAN) imagery, RGB inager

16. SECURITY CLASSIFICATION OF: a. REPORT	b. ABSTRACT	c. THIS PAGE	17. LIMITATION OF ABSTRACT	18. NUMBER OF PAGES	19a. NAME OF RESPONSIBLE PERSON
				2	Beverly Walters
					19b. TELEPHONE NUMBER *(Include area code)* 813-866-3374, ext. 101

IMPACTS/APPLICATIONS

The abilities to detect targets and characterize the environment in the Very Shallow Water (VSW) and beach zone are critical to MIW, MCM, and NSW operations. The image fusion techniques here will provide enhanced abilities to detect and characterize target in access denied areas using both geomorphology (shape) and spectral (color) signatures. In addition, the successful development of these techniques will feed back into the development of new imaging systems for space and aircraft platforms, including Unmanned Aircraft Systems (UAS).

This work demonstrated the ability to fuse high resolution multispectral imagery with lower resolution hyperspectral imagery using a new method of color tinting fusion. On simulated multispectral imagery we achieved a ~6% reconstruction error across the VNIR spectrum; on actual multispectral imagery we achieved ~20% reconstruction error. The difference between the simulated and actual was mostly attributed to the inability to calibrate and atmospherically correct the multispectral imagery.

Microwave imagers are typically Synthetic Aperture Radar (SAR). While the field has been generally confined to airborne and space-based platforms, imagery data fusion may also include some combination of data from these platforms with data from in-water systems such as multibeam and side-scan sonar imagery. In short, data fusion is the process by which two or more streams of data of different temporal and spatial resolution are combined to produce synthesized products which are unattainable from a discrete image.

The advantages of data fusion are fairly clear. In the temporal domain, data fusion allows for the more complete imaging of an area intermittently covered by clouds. It may also provide better analysis of movement or time-dependent change in targets and/or environmental conditions. In the electromagnetic frequency domain, targets which are visible in one image type may be less than visible in another, and vice versa. SAR imagery may illuminate target elevations or directional wave spectra, whereas optical imagery may identify targets by shape and color. Combining the targeting and identification of these different data types provides target recognition and environmental characterization with high confidence and lower false alarm rates than may be found from single source imagery. In the spatial domain, objects that are identifiable on the basis of size and shape in panchromatic (PAN) imagery are often unidentifiable by their geometric dimensions in lower resolution multispectral or hyperspectral imagery. The converse is that the spectral imagery provides the ability to identify targets or characterize the environment based on unique spectral signatures, which is unavailable in the panchromatic imagery, but may not be able to resolve the shape or dimensions of small targets.

This project seeks to co-locate simultaneously collected MSI/HSI data streams to develop enhanced imagery sharpening capabilities for use in target detection and environmental characterization. It seeks to build upon PAN sharpening techniques by using the full spectral information provided by MSI data streams. We hypothesize that the best way to attempt this image fusion is at the level of remote sensing reflectance, so the MSI data must be corrected for illumination and atmospheric interference. The spectral information from the co-registered MSI/HSI Rrs data will then be fused to provide more accurately sharpened HSI data for spectral target algorithms.

WORK COMPLETED – Year 1

This project began in April of 2005, and started with data previously collected by FERI. FERI, in collaboration with the California State University System, under the NOAA-funded California Center for Integrative Coastal Observation, Research and Education (CICORE) Program (http://www.feriweb.org/projects/ci-core/) recently (Fall 2004) collected over 5,000 square kilometers of 0.3 meter MSI and 3 meter HSI data over a wide variety of coastal environments along the California coast (http://www.feriweb.org/projects/ci-core/arcims/). The survey sites include Humbolt Bay, San Francisco Bay, Monterey Bay, the Big Sur coast, San Luis Bay, Santa Barbara, Newport, and San Diego Harbor. The MSI instrumentation was provided under a cooperative agreement with the Applanix Systems Integration Group (ASIG), a subsidiary of the Trimble Corporation. This MSI system (Digital Sensor System; http://www.applanix.com/products/dss_index.php) was provided as part of the Applanix Position and Orientation System (POS AV; http://www.applanix.com/products/posav_index.php), which was being evaluated as a replacement for the current POS system on the NRL PHILLS 2 airborne hyperspectral imager.

The raw DSS imagery (MSI imagery) and POS data was provided to FERI by ASIG after the flights. The processing and geo-positioning of the MSI data was completed by FERI under this ONR project.

This geo-positioning system is of much greater accuracy than the previous POS system on the PHILLS 2. The processing of this POS data stream required additional training, which was provided by ASIG. In addition, the DSS is a frame camera imagery, which is very different from the line scanning imager, which is at the heart of the PHILLS 2. The processing of the MSI data stream itself required additional training in the photogrammetry and ortho-rectification. The training was completed, as well as the processing of the raw POS data and DSS imagery to ortho-rectified (Figure 1). These data are to be used with the co-registered HSI data from the Morro Bay region (Figure 2).

Figure 1. FERI MSI of selected region in Morro Bay, CA collected November 11, 2004. This area has been chosen as a focus site for the development of the MSI/HSI fusion algorithms. Note the enhanced spatial resolution when compared to the HSI imagery in Figure 2.

RESULTS – Year 1

The MSI/HSI data has been co-registered in anticipation of the next step in the development of the spectral fusion over the next 6 months. One issue that has been found during the training of FERI personnel by ASIG, which may be cause for difficulties, is that the radiometric and spectral calibrations of the DSS are not what have been purported by the manufacturer. The calibration issues need to be resolved prior to the development of the Rrs fusion approach, for it will be very difficult to correct for illumination and atmospheric effects without accurate calibration. This recalibration of the MSI sensor by FERI personnel is scheduled to occur this fall (funded by Trimble), so these data should be available later this year to complete the initial development of the Rrs fusion approach.

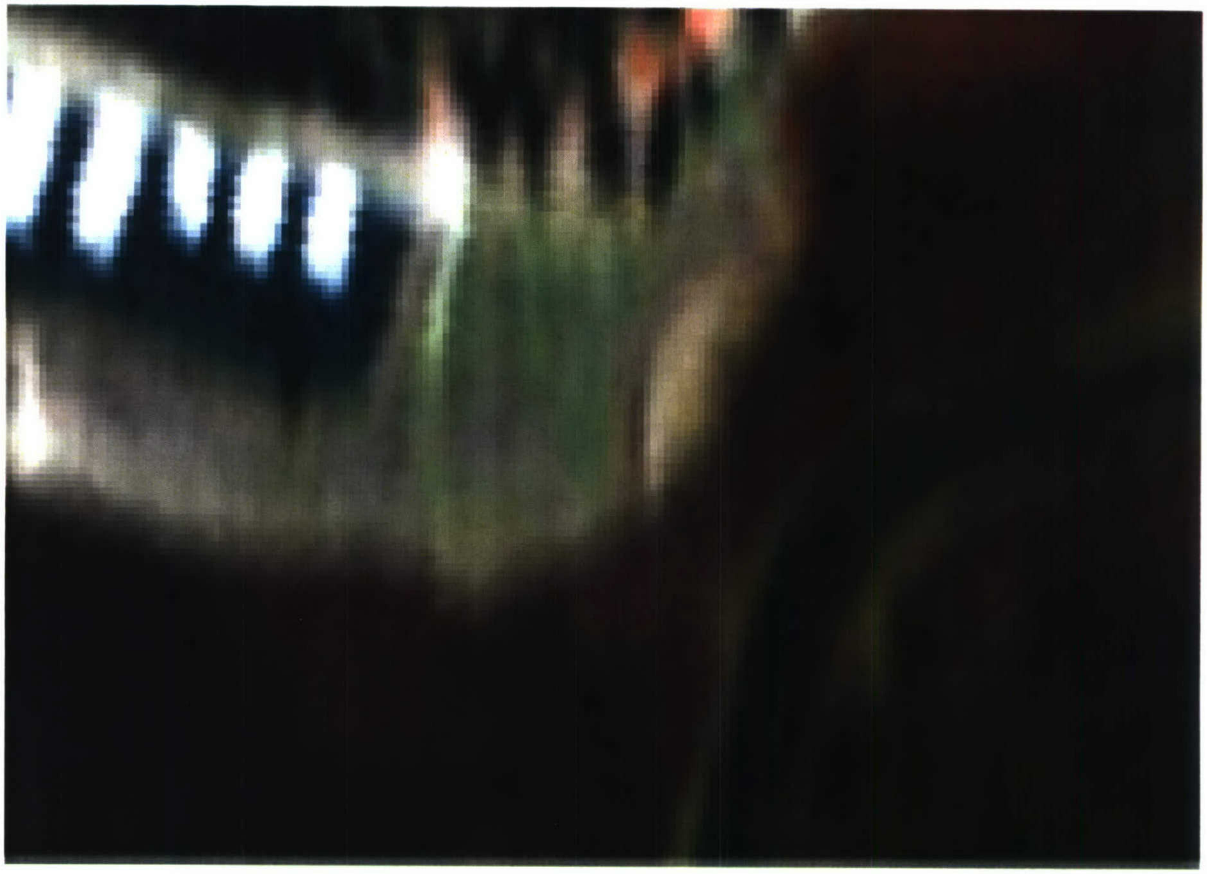

Figure 2. FERI HSI of selected region in Morro Bay, CA collected November 11, 2004. This area has been chosen as a focus site for the development of the MSI/HSI fusion algorithms. Note the reduced spatial resolution when compared to the MSI imagery in Figure 1.

WORK COMPLETED – Year 2

The work during this period looks at exploiting the information available from multiple sensors aboard an aircraft. Particularly, we wish to combine information from a high spatial but low spectral resolution camera and a low spatial but high spectral resolution camera. The desired final image should have both, high spatial and high spectral resolution. Data fusion can be defined as the fusion of complementary information from multiple sources. In this work, we focus on the combination of low-resolution multi-spectral data with high-resolution tri-band (RGB) data. Many image fusion techniques have been proposed to merge multi-spectral (MS) and panchromatic (Pan) images, with complementary characteristics of spatial and spectral resolutions. They are mostly component substitution based methods such as IHS, Brovey and MULTI.

The IHS (Intensity, Hue, and Saturation) transformation is mostly used for three band images. In the IHS transformation, the difference between the high resolution and low resolution intensity images is added to the up-sampled MS bands. However, as the spectral response of the two cameras is usually different, this procedure is prone to spectral distortion. When more than three bands are present, this transformation can be applied to groups of three consecutive bands at a time. Alternatively, a PCA (Principal Component Analysis) approach can be used.

The Brovey fusion method computes the ratio between a panchromatic cell value and the average of the corresponding multi-spectral cell values and uses that ratio to compute the final color component values for the pan-sharpened image. The Gram-Schmidt (GS) technique is another component substitution technique for spectral sharpening. In the GS method, the low-resolution version of the PAN image is obtained as the pixel average of the MS bands. However, as discussed earlier, because of the radiometric differences between the two sensors, the reconstructed image is prone to suffer from spectral distortion. The purpose of this work is to mitigate this distortion by reconciling the two sensors radiometrically, prior to performing the GS fusion. A similar approach is taken in *Aiazzi et al, 2006* where regression coefficients are determined to reconcile the two sensors prior to GS sharpening. In our case, however, the sensor response is known a priori, obviating the need for determining coefficients.

RESULTS – Year 2

The purpose of this work is to construct a high spatial and high spectral resolution image using images from two sensors. One sensor is a high spatial resolution frame camera – the DSS-322. The other is a high spectral resolution camera, FERI's SAMSON. The Gram Schmidt procedure described above was used to combine information from the two cameras to obtain a high spectral, high spatial resolution image.

To evaluate the validity of the reconstructed image, the hyper-spectral and multi-spectral images had to be down-sampled spatially and then used to reconstruct the original hyper-spectral image. The error between the reconstructed and original hyper-spectral image is a quantitative indicator of the proposed procedure's validity.

Image fusion was studied under two conditions – practical and ideal. In the practical scenario, actual hyper-spectral and multi-spectral images were used. For the ideal scenario, an actual hyper-spectral and a simulated multi-spectral image (simulated using the hyper-spectral image) were used. By using hyper-spectral and multi-spectral images derived from the same sensor, many error sources such as registration, calibration and atmosphere are eliminated. Comparing results from these two scenarios helps quantify the error contribution from these sources.

The simulated DSS image was obtained from the hyper-spectral image using the spectral response function of the DSS camera. Each band of the DSS camera was simulated by taking a dot product between that band's spectral response function with the actual wavelength responses from the hyper-spectral signal as shown in Equation 1.

$$DSS(i,j,k) = \sum_{\lambda=\lambda_{\min}}^{\lambda_{\max}} HYP(i,j,\lambda) \times SRF_k(\lambda) \qquad (1)$$

Here, k indicates the DSS's band, k={1,2,3}, (i,j) indicate the pixel location, $SRF_k(\lambda)$ is the kth band's response at wavelength λ.

Two approaches to image fusion were compared. In the first approach, GS was run using the hyper-spectral image and one of the DSS bands to obtain the reconstructed hyper-spectral image as shown in Figure 3.

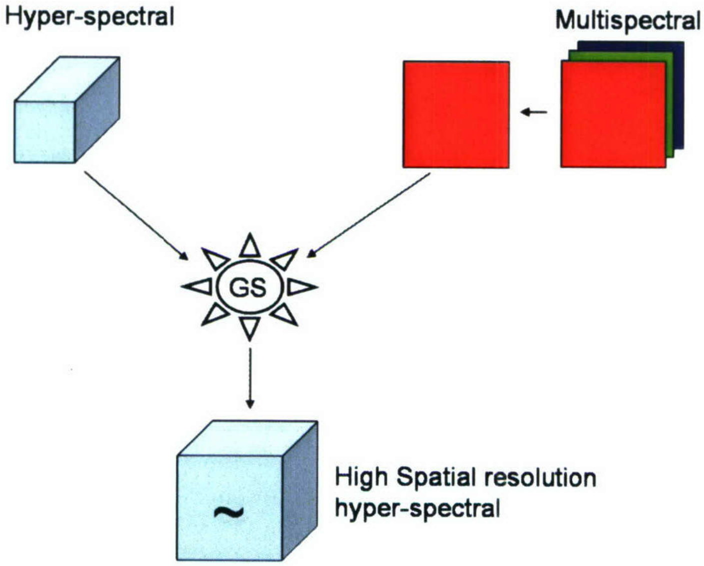

Figure 3. In the traditional Gram-Schmidt approach a single PAN channel is used to fuse the high spatial resolution with the lower spatial, but high spectral resolution image.

In the second approach, the hyper-spectral image was multiplied by each band's SRF response, to obtain three 'tinted' hyper-spectral images. Three reconstructions were performed to obtain 'tinted' reconstructed images. They were then multiplied by the corresponding inverse SRF response to obtain three versions of the original hyper-spectral image. Figure 2 illustrates how a hyper-spectral image was generated using the red channel.

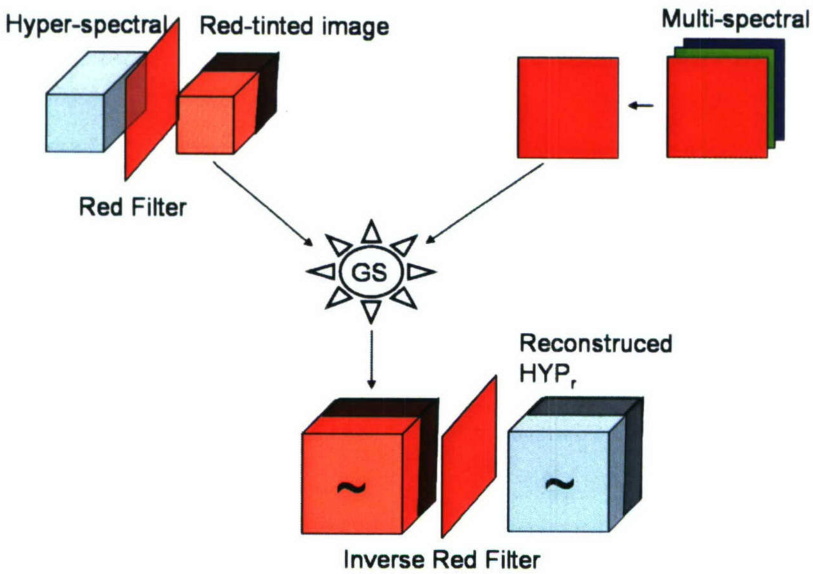

Figure 4. In the modified Gram-Schmidt approach each RGB channel is used only with the overlapping bands in the HSI image cube.

Tinting the image prior to using the GS, ensures that the hyper-spectral and multi-spectral images have similar spectral content leading to better reconstruction. Once three versions of the reconstructed hyper-spectral image are obtained, they can be averaged to obtain a final reconstructed version. In this work, a more elegant fusion scheme was used as shown in Equation 2.

$$HYP_{avg}(\lambda)=W_r(\lambda)HYP_r(\lambda)+W_g(\lambda)HYP_g(\lambda)+W_b(\lambda)HYP_b(\lambda) \qquad (2)$$

Where $Wr(\lambda) = SRFr(\lambda) / (SRFr(\lambda) + SRFg(\lambda) + SRFb(\lambda))$. This means that instead of weighting the three images equally (as you would in an average), they are now weighted in proportion to their dominance at each wavelength.

DISCUSSION – Year 2

In this section, we compare the performance of the modified method to that of the original method in the ideal scenario. Then, we compare our method's performance in the two scenarios (ideal and practical). This is followed by a detailed discussion of the results.

First we evaluate the efficacies of the proposed modified method and the original method in the ideal scenario. Figure 3 and Figure 4 described the workings of the two methods. A three band multi-spectral image was simulated from the hyper-spectral image as described by Equation 1. The original hyperspectral image was reconstructed using both methods and the errors were evaluated.

To characterize the nature of the reconstruction error, we studied its distribution along wavelengths and magnitudes. The error is expressed as a fraction of the original hyper-spectral image.

Figure 5 shows the reconstruction errors in the ideal scenario using both methods. The X-axis ranges from band #40 to band #80 spanning wavelengths from 400nm to 700nm. The Y-axis expresses the error as a fraction of the original value. From (a), it is evident that the reconstruction error using Method 1 is in the 15-20% range. From (b), it can be seen that using the Tinting method, the error drops to the 6-8% range.

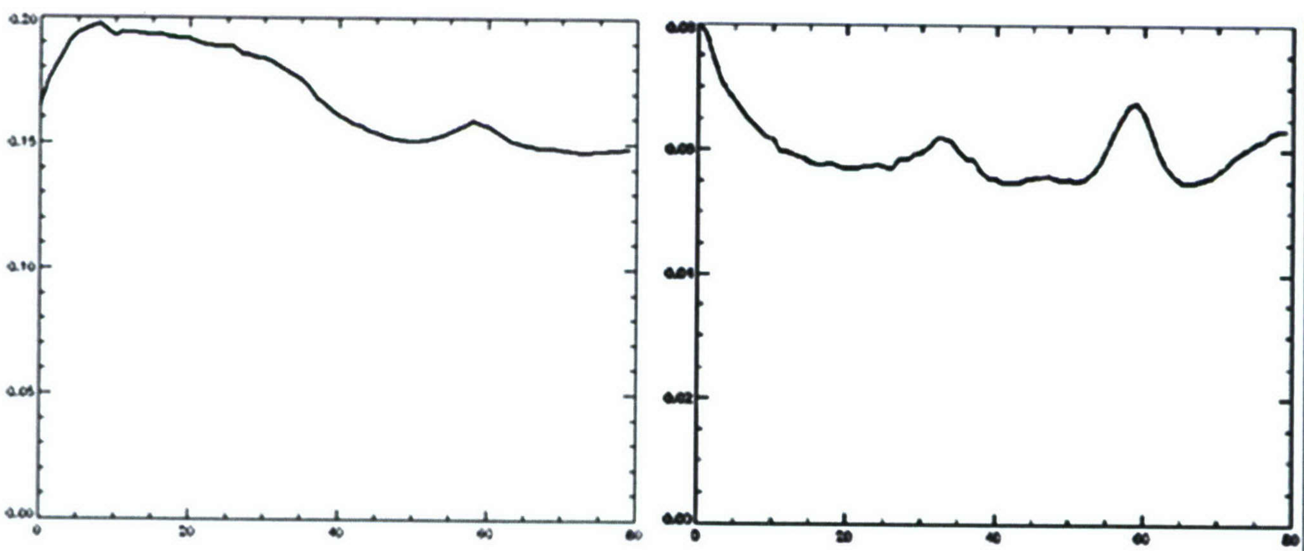

Figure 5. The graph on the left shows the errors in the ideal comparison case using the traditional Gram-Schmidt approach, and the range is ~15-20% over the spectrum. In the modified color tinted, Gram-Schmidt approach (right graph) there is a marked reduction in the reconstruction error, range is ~6-8% over the spectrum.

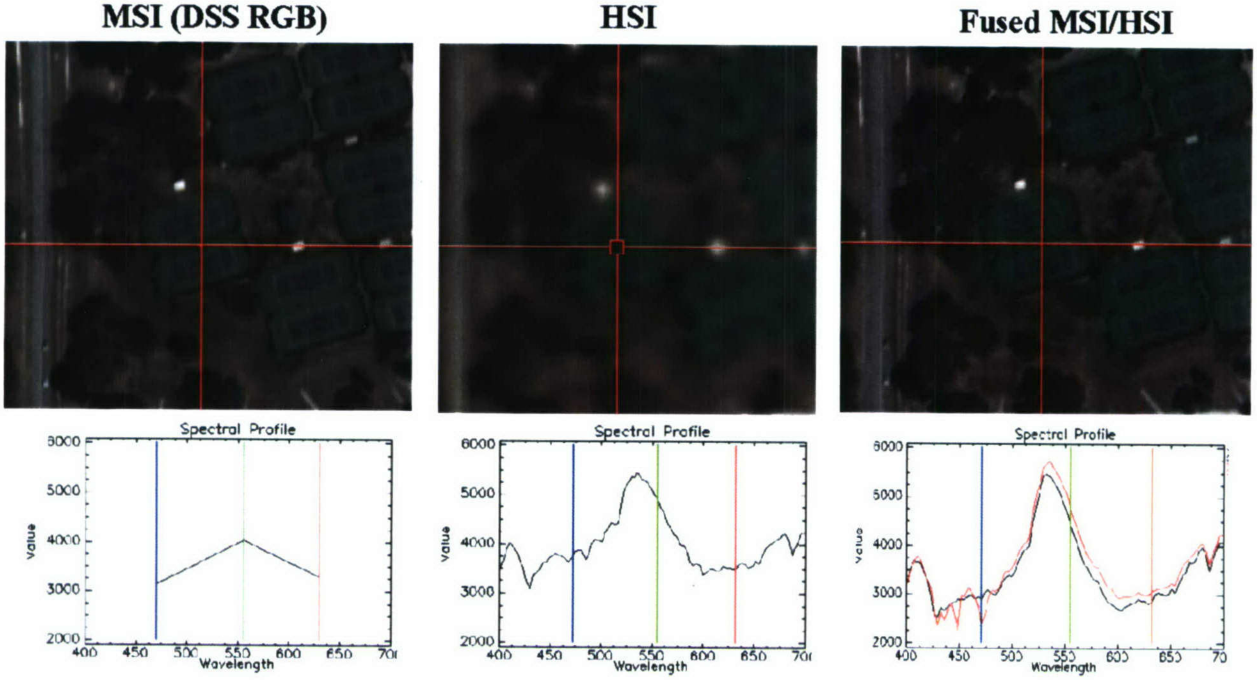

Figure 6. The color tinted fusion of high spatial resolution MSI (left figure) with lower spatial resolution HSI (middle figure) into a high spatial resolution, high spectral resolution image (right image). The bottom row of images represents the spectral plots at the pixel located at the center of the red cross hairs in the images directly above them.

Next we compare the reconstruction errors in two different scenarios using the Tinting method. Figure 7 compares the errors in the ideal and practical scenarios.

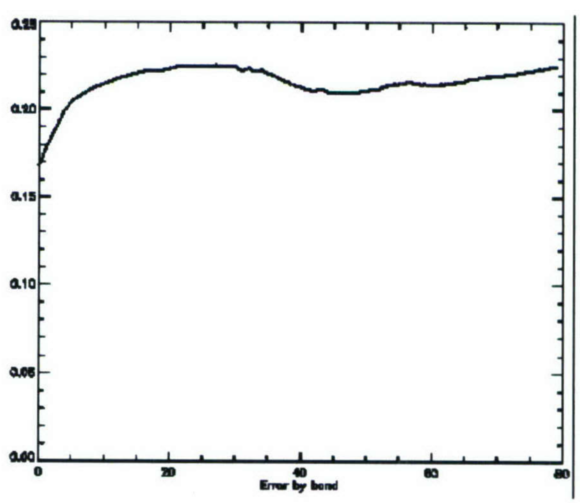

Figure 7. This graph shows the reconstruction error in the practical case, where the DSS imagery is used in the modified Gram-Schmidt approach to fusing the MSI/HSI data. The increase in the error range to ~22% results from differences in (1) the unknown calibration of the DSS, (2) view angle and its impacts on atmospheric and illumination contamination, and (3) pixel co-registration errors.

From Figure 7, it is evident that as we move from the Ideal to the Practical scenario, the average error jumps from about 5% to 22.5%. There are multiple reasons for this jump in reconstruction error as we move from the Ideal to Practical scenarios.

First, errors arise because the multi-spectral camera is not accurately calibrated. We have sought to work with the manufacturer to resolve these calibration issues, but as of yet, this sensor can not be calibrated to any radiometric standard.

Second, the two sensors look at the same location through different view angles, the hyper-spectral camera view is nominally at a nadir angle in the along track direction, and ~+/-20 degrees in the cross track direction (pushbroom type sensor), whereas the multi-spectral camera usually looks at an angle varying from 0-20 degrees in both the along track and cross track directions (framing type sensor). Thus their path lengths through the atmosphere and each pixels relative illumination are different, which yield a different overall spectral signal between the DSS and SAMSON when the data are not corrected for atmospheric and illumination differences.

Third, since two cameras have different resolution and lens aberration, image registration is inaccurate. It was observed that a registration error of one pixel can contribute up to 5% error.

We hypothesize that of the 20% average error, errors due to atmosphere and calibration account for 10% of the error, 5% due to image mis-registration and the remaining 5% is inherent in the GS procedure. In spite of the errors, this approach shows great promise in being able to generate HSI data at the spatial resolution of PAN and RGB imagers. We need to cross the critical step of calibrated the RGB/MSI data so that we may apply this technique to the reflectance data itself, rather than the sensor radiance data. This would greatly reduce the errors in the Practical Approach shown here, allowing us to approach our 5% reconstruction error seen in the Ideal Approach.

IMPACTS/APPLICATIONS

The abilities to detect targets and characterize the environment in the Very Shallow Water (VSW) and beach zone are critical to MIW, MCM, and NSW operations. The image fusion techniques here will provide enhanced abilities to detect and characterize target in access denied areas using both geomorphology (shape) and spectral (color) signatures. In addition, the successful development of these techniques will feed back into the development of new imaging systems for space and aircraft platforms, including Unmanned Aircraft Systems (UAS).

This work demonstrated the ability to fuse high resolution multispectral imagery with lower resolution hyperspectral imagery using a new method of color tinting fusion. On simulated multispectral imagery we achieved a ~6% reconstruction error across the VNIR spectrum; on actual multispectral imagery we achieved ~20% reconstruction error. The difference between the simulated and actual was mostly attributed to the inability to calibrate and atmospherically correct the multispectral imagery.

RELATED PROJECTS

This project works closely with those of PIs Bissett and Kohler, including N000140110201, N000140310626, and N000140410297

REFERENCES

Aiazzi, B., Alparone, L., Baronti, S. and Selva, M., 2006. MS + Pan Image Fusion by an Enhanced Gram-Schmidt Spectral Sharpening, 26th Symposium of the European Association of Remote Sensing Laboratories (EARLSeL), Warsaw, Poland.

Pohl, C. and Genderen, J.L.V., 1998. Multisensor image fusion in remote sensing: concepts, methods and applications. International Journal of Remote Sensing, 19(5): 823-854.